A review of basin-wide calcareous nannofossil bioevents in the Mediterranean at the onset of the Messinian Salinity Crisis

Francesca Lozar[1] and Alessandra Negri[2]

Published on Marine Micropaleontology, 10.1016/j.marmicro.2019.101752

Corresponding author: Francesca Lozar (francesca.lozar@unito.it)

1 Dipartimento di Scienze della Terra (Earth Sciences Department), Università degli Studi di Torino, Via Valperga Caluso, 35, 10125 Torino, Italy.

2 Dipartimento di Scienze della Vita e dell'Ambiente (Dept. of Life and Environmental Sciences) Università Politecnica delle Marche, via Brecce Bianche, 60131 Ancona, Italy.

Abstract

During the Messinian (7.2 to 5.3 Ma) the Mediterranean area experienced fast and deep climatic and eustatic structural changes. The stratigraphic framework for this interval is relatively well constrained and the beginning of the Messinian salinity crisis (MSC) dated at 5.971 Ma suggests a duration of at least 1.2 Ma for the pre-evaporitic Messinian that is the object of this study.

Several sites (Faneromeni, Pissouri, Polemi Basin, Kalamaki, Falconara, Fanantello, Lemme, Pollenzo, Govone, Moncalvo: Blanc-Valleron et al., 2002; Wade and Bown, 2006; Kouwenhoven et al., 2006; Morigi et al., 2007; Lozar et al., 2010, 2018; Dela Pierre et al., 2011, Karakitsios et al., 2017) show similar behaviour of the calcareous nannofossil record where several peaks of *Sphenolithus* spp. are recognized at different levels in each of the section.

This paper compares the calcareous nannofossil data from six different sections across the Northern and Eastern Mediterranean area encompassing the onset of the MSC.

Interestingly, a tight succession of bioevents (*Sphenolithus abies*, *Helicosphaera carteri*, *Umbilicosphaera rotula*, *Rhabdosphaera* spp.) is recorded in all the sections analyzed and appear to correlate precisely among the investigated sites, approximating the onset of the Messinian salinity crisis, thus offering the possibility to use these as bioevents for regional correlation.

Keywords: calcareous nannofossils, biostratigraphy, Mediterranean Sea, Messinian Salinity crisis.

1. Introduction

During the Messinian (7.2 to 5.3 Ma) the Mediterranean area experienced fast and deep climatic and eustatic structural changes.

The interval preceding the Messinian salinity crisis (MSC) was characterized by marked paleoceanographic changes culminating in the deposition of a huge volume of evaporites in the shallow and deep/intermediate settings of the Mediterranean Basin during 3 stages: 1) from 5.971 Ma, 2) from 5.6 Ma and 3) from 5.55 Ma (Manzi et al., 2013; Roveri et al., 2014, with references therein). However the evidences of the oceanographic crisis were apparent well before starting at 7.16 Ma with further steps at 6.7, 6.4 and 6.1 - 6.0 Ma (see Gennari et al., 2018; Kouwenhoven et al., 2006, with references therein). Each of these steps conducted to increasingly stressing conditions both at the sea floor and in the water column, as documented by the progressive increase of oligotypic calcareous plankton and benthic foraminifer

assemblages. The first two steps (7.16 and 6.7 Ma) were related to the tectonic narrowing and/or closure of the Atlantic connections in the Gibraltar region (Flecker et al., 2015; Krijgsman et al., 2018, and references therein), which caused the slowing or even stopping of the Mediterranean deep circulation. In fact during the early Messinian, the Mediterranean-Atlantic connections through the Betic and the North Rifian Corridor were closed by Africa-Iberia convergence processes and the Gibraltar Strait was the sole open connection to the Atlantic ocean (Krijgsman et al., 2018). At the base of the Messinian the benthic fauna was the most affected, as demonstrated by the slight impoverishment of the assemblage diversity (Kouwenhoven et al., 2006). In such a framework, the Precession-controlled cyclic deposition of sapropels and diatomite beds started, as recorded as early as 6.98 Ma in Sicily (Blanc-Valleron et al., 2002) and at about 6.7 Ma in the Western (Sierro et al., 2003) and Eastern Mediterranean (Kouwehoven et al., 1999, 2006; Morigi et al., 2007). At this time also the calcareous plankton was characterized by reduced diversity and abundance (Blanc-Valleron et al., 2002; Sierro et al., 2003; Kouwenhoven et al., 2006). Noteworthy, the changes in the calcareous plankton assemblages equally affected both deep and shallow water successions.

From 6.4 Ma a further synchronous change in the water mass is evidenced by the microfossil record: the Plankton/Benthos ratio shows abrupt fluctuations, with values ranging from 100% to near 0%, indicating the occurrence of abenthic foraminiferal layers, possibly due to anoxic bottom water conditions during insolation maxima, and of strongly reduced/aplanktonic layers at insolation minima (Blanc-Valleron et al., 2002; Gennari et al., 2018; Kouwenhoven et al., 2006; Sierro et al., 2001, 2003). In the superficial waters, the presence of oligotypic assemblages dominated by *Turborotalita quinqueloba* and *T. multiloba* (up to 80%) during insolation minima are

usually related to increased salinity corresponding to very arid climatic phases (Kouwenhoven et al., 2006; Sierro et al., 2003).

Between 6.1 - 6.0 Ma, the final decrease of calcareous microfossils starts, whose disappearance is regarded as a good proxy for the MSC onset at 5.971 Ma (Manzi et al., 2007; Lozar et al., 2010; Manzi et al., 2011, 2013; Gennari et al. 2013, 2018; Violanti et al., 2013), despite some sections are barren of calcareous plankton well below the 5.971 Ma timeline (Catalano et al., 2016; Dela Pierre et al., 2016).

The chronostratigraphic framework of the Mediterranean Messinian is in general well constrained on the basis of both planktonic foraminifer and calcareous nannofossil biostratigraphic datums. In fact, the identification of the Messinian stage is currently given by the calcareous plankton bioevent *Globorotalia miotumida* FCO (dated at 7.246 Ma) and approximated by the *Amaurolithus delicatus* FAD (at 7.134 Ma) in chron C3Bn (Hilgen et al., 2000).

Several biostratigraphic studies have been conducted in the last two decades (Negri et al.,1999, Negri and Villa, 2000, Morigi et al., 2007 among others) evidencing that in the Mediterranean region, the *Amaurolithus* species are rare or very rare, but they are consistently recorded and used for biostratigraphic purposes (Raffi et al., 2003). The appearance of *A. primus* was astronomically dated at 7.43 Ma (Negri and Villa, 2000), which is in agreement with the calibration in equatorial regions and the Metochia section (Greece; Raffi et al., 2003). In the Mediterranean area, the *A. delicatus* FO was generally recorded well above the *A. primus* FO (i.e., Flores et al., 1992; Negri et al., 1999), i.e., close to the first regular occurrence of the planktonic foraminiferal *Globorotalia miotumida* Jenkins 1960 group and thus close to the Tortonian- Messinian boundary (Hilgen et al., 2000). Hence, the *A. delicatus* FO was considered the nannofossil biohorizon that best approximates the boundary. In

addition, the *A. delicatus* FO biohorizon, as defined in the Mediterranean, has no biostratigraphic value since outside this area, the appearance of *A. delicatus* coincides closely with the appearance of *A. primus*. Any further stratigraphic detail in the Mediterranean Messinian relies upon the *N. amplificus* FO (marking the lower boundary of subZone MMN11c, Raffi et al,. 2003) and LO bioevents (6.689 and 6.141 Ma respectively), but this taxon is overall very rare and thus of minor biostratigraphic value. Moreover, *Amaurolithus* spp., an extinct taxon flourishing in warm oligotrophic waters, is often very rare in the frame of a meso-eutrophic late Miocene ocean (Drury et al., 2018: Late Miocene Biogenic Bloom); the *Amaurolithus* spp. abundance was probably adversely affected by the high nutrient waters characterizing the Mediterranean during the Messinian, at least since 6.98 Ma, as testified by diatomite occurrence and high organic matter content across the basin (Pellegrino et al., 2018, and references therein). An additional bioevent is the continuous occurrence of the taxon *Reticulofenestra rotaria*, which total range has not been precisely investigated, but which occurs at least in the interval 7.2 to 6.4 Ma (Theodoridis, 1984, Young, 1998, Raffi et al., 2003), and spans subzone MMN11b.

As said above, the Mediterranean marine paleobiological record is characterized by the occurrence of progressive changes throughout the entire Messinian, testifying to the stepwise restriction of hydrographic connection between the Mediterranean Sea and the world's oceans, that finally lead to the onset of the Messinian salinity crisis (MSC) at 5.971 Ma (Manzi et al., 2013; Flecker et al., 2015). This means that between 7.1 Ma and 5.971 calcareous nannofossil biostratigraphy is of poor utility and stratigraphy in this interval relies mainly on planktonic foraminifer datums (see Gennari et al. 2018 and references therein) and on different stratigraphic techniques, such as magnetostratigraphy, cyclostratigraphy (Krijgsman et al. 1999; Krijgsman,

2002; Ochoa et al., 2015), well-logging (Van den Berg et al., 2018), physical stratigraphy (Lugli et al., 2010, Dela Pierre et al., 2011), and chemostratigraphy (Bellanca et al., 2001, Blanc-Valleron et al., 2002). Several planktonic foraminiferal bioevents are regarded as well-established and synchronous at the basin scale (Sierro et al. 2001, Gennari et al. 2018), but fail to identify the onset of the MSC, the main oceanographic event at the regional scale. In general, the disappearance of calcareous plankton is regarded as a synchronous event and a reliable proxy for the onset of the MSC, and often used as a stratigraphic constraint (see Sierro et al., 2001, 2003; Gennari et al. 2013, 2018, for more details), but this is not always the case and the record of several sections shows that this event is diachronous even over short distances (Violanti et al., 2013; Catalano et al., 2016; Dela Pierre et al., 2016). Moreover the upper part of the Messinian interval (within the 5.97- 5.33 Ma interval), which falls entirely within the lower part of the Gilbert reverse chron, due to scattered fossil content, has been defined as a “non-distinctive zone” on the ground of planktonic foraminifera (Iaccarino and Salvatorini, 1982).

Here we will review the published data relative to six sections encompassing the MSC deposits, where a peculiar succession of local calcareous nannofossil events of the species *Sphenolithus abies*, *Helicosphaera carteri*, *Umbilicosphaera rotula* and *Rhabdosphaera* spp. appear to be useful to approximate the MSC onset.

In further detail, our manuscript reports the data from different sections in the Mediterranean area from the Piedmont Basin (Italy; Pollenzo, Banengo, Moncalvo, Lozar et al., 2018), from the Vena del Gesso Basin (Italy; Fanantello, Manzi et al., 2007, and new data reported in the present paper) and from Cyprus (Pissouri, Kouwenhoven et al., 2006; Morigi et al., 2007, and Tokhni, Gennari et al., 2018). The sections are characterized by the alternation of sapropel/marl/shale beds, and

marl/carbonate beds; this sharp lithologic cyclicity, driven by climatic precession (Krijgsman et al., 1999; Roveri et al., 2014 and references therein) allowed the direct tuning of the sections to the Laskar et al. (2004) insolation curve, thus providing a strong and very detailed chronostratigraphic framework useful to correlate the abundance peak of the species investigated in this work.

2. Material and methods

The six sections considered for this work span the interval recording the onset of the MSC (Fig. 1). The data presented here are already published, except for the Fanantello section, where additional information on the distribution of *H. carteri* and *Rhabdosphaera* spp. are provided, together with data on Sphenolith distribution already reported in Manzi et al. (2007). Samples were prepared as simple smear slides (Bown and Young, 1998) and counting of at least 300 specimens was performed to obtain raw data later transformed as percentages of the total assemblage.

We will present the data from west to east, and the new data obtained will be added to those already published.

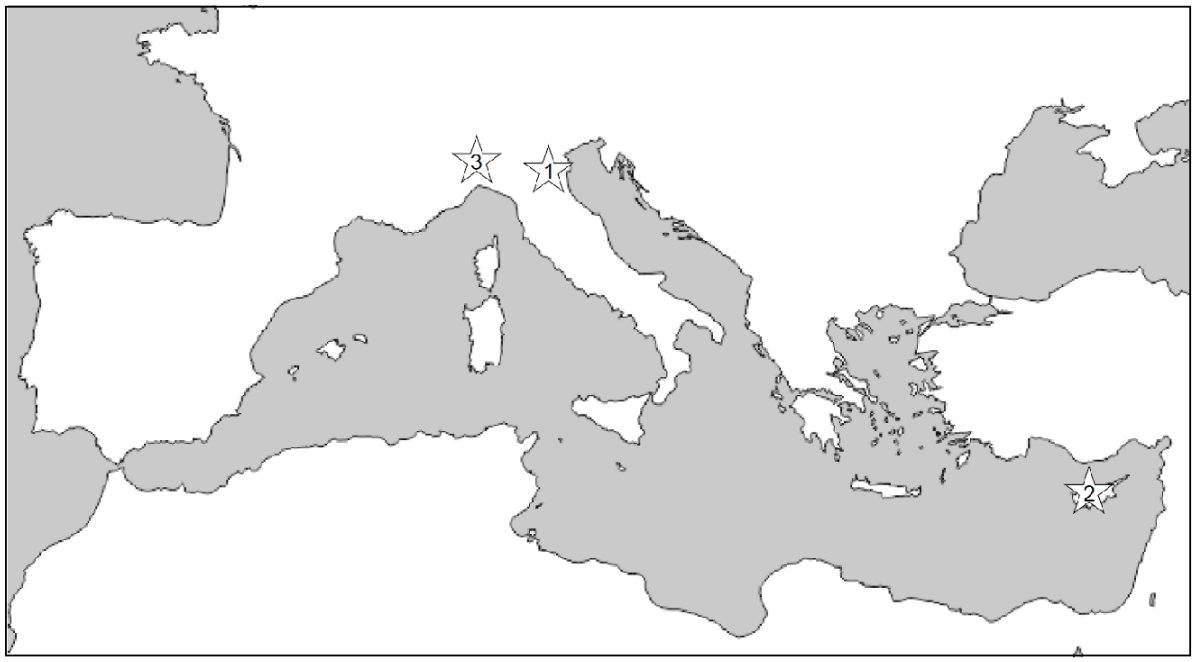

Fig. 1. Geographic location of the studied sections. 1: Fanantello, Northern Apennines (Italy); 2: Tokhni and Pissouri, Cyprus; 3: Pollenzo, Banengo and Moncalvo, Piedmont Basin (Italy).

3. The data

In the Piedmont Basin (PB, Italy), at the northern edge of the Mediterranean, the three sections Pollenzo, Banengo, and Moncalvo (Fig. 2) show similar lithologic cyclicity (shale/marl or shale/limestone cycles); the sediments are characterized by moderate to poorly preserved CN assemblages dominated by *Reticulofenestra* spp.. The three sections are characterized by the presence of a remarkable *S. abies* peak abundance in the shale bed of the lithologic cycle correlative to the first gypsum cycle deposited on the basin margins (PLG1; Roveri et al., 2014 and references therein), where the base of the gypsum has been dated at 5.971 (Manzi et al., 2013). The amplitude of this peak differs from section to section (60% at Pollenzo, 64% at Banengo, 10% at Moncalvo), but the event is easily detected since much lower abundances are recorded below or above this bed (Lozar et al., 2018). Remarkably,

also *H. carteri* shows a sharp increase in abundance in all the three sections just above (30% Pollenzo and Banengo) or simultaneously (6% in Moncalvo) with the *S. abies* peak. Noteworthy, at Pollenzo two additional taxa, *Rhabdosphaera* spp. and *Umbilicosphaera rotula*, also increase in abundance just above the *S. abies* peak. *Rhabdosphaera* spp. are very rare across the section, but they increase to 13% just above the *S. abies* peak in cycle Pm5. As for *U. rotula*, it shows an abundance peak in the gypsum-equivalent bed in Pollenzo (70% in the topmost Pm5 cycle; Fig.2). All these peaks (Fig. 2) are clearly identified, since *S. abies*, *H. carteri*, *U. rotula*, and *Rhabdosphaera* spp. show an overall low relative abundance below and above this cycle (Lozar et al., 2010; Dela Pierre et al., 2011; Violanti et al., 2013; Lozar et al., 2018) in the section.

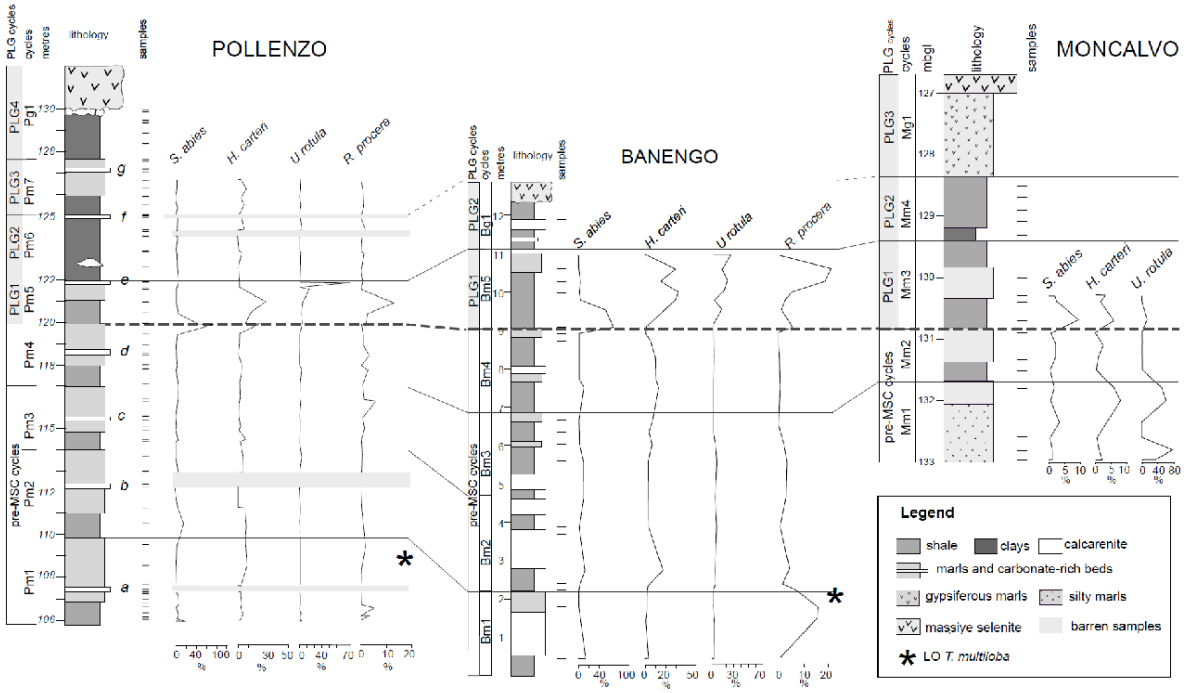

Fig. 2. Selected calcareous nannofossil relative abundances and correlation of the Piedmont Basin sections by means of calcareous nannofossil and planktonic foraminifer datums (Data from Lozar et al., 2018).

At the Banengo section the succession of events occurs at the same stratigraphic position as in Pollenzo although with different frequencies (22% for *Rhabdosphaera* spp., 23% for *U. rotula)*. Instead, the Moncalvo section record is less straightforward: both the *S. abies* and *H. carteri* peaks are recorded, albeit with lower abundances than the previous sections, together with a minor *U. rotula* (6%) peak; *Rhabdosphaera* spp. are virtually absent, never exceeding 1% of the total assemblage (not figured). This record differs from the other sections in having a very high abundance of diatoms, that could account for the overall low abundance of calcareous nannofossils and the very high abundance of small *Reticulofenestra* (not shown), well adapted to the high nutrient input that made diatoms flourish.

Moving southeastward, in the Fanantello section (Northern Apennines, Italy), the interval spanning the MSC onset consists of thin-bedded turbidites (111-55 m) passing towards the top to euxinic shales, limestone and thin-bedded turbidites (55-0 m), without a distinct cyclic pattern. This interval (6.17-5.60 Ma, Manzi et al., 2007) show calcareous nannofossil decreasing abundances and also reduction in biodiversity, since discoasters disappear. In addition, in the upper part of this interval, clear peaks of *S. abies* have been recorded.

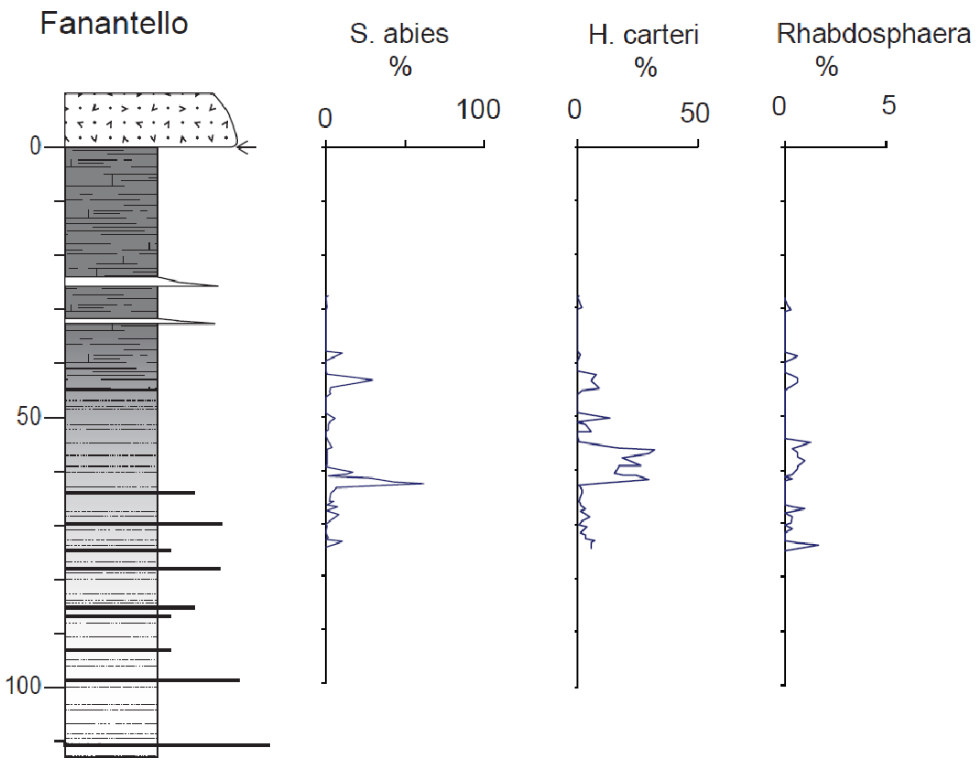

Fig. 3. Selected calcareous nannofossil relative abundance for the Fanantello section.

Above the foraminifer last recovery, at 61 m, the succession is characterized by rare autochthonous nannofossils (mainly *S. abies*) with rare occurrence of *H. carteri,* small *Reticulofenestra* spp. and barren intervals. Three main peaks of *S.abies* have been recorded by Manzi et al. (2007) at 62.77 m, 43.44 m, and 38.47 m depth respectively. In the first peak *S. abies* represent up to the 62% of the whole assemblage; Figure 3 reports new data and shows an abundance increase of the taxa *H. carteri* and *Rhabdosphaera* spp. just above the first and most relevant *S. abies* peak, at 62.77 m. *Umbilicosphaera* spp. were not recorded in this section.

Finally, in the Eastern Mediterranean, the sections from Cyprus (Pissouri and Tokhni), also show a comparable succession of events (Fig. 4).

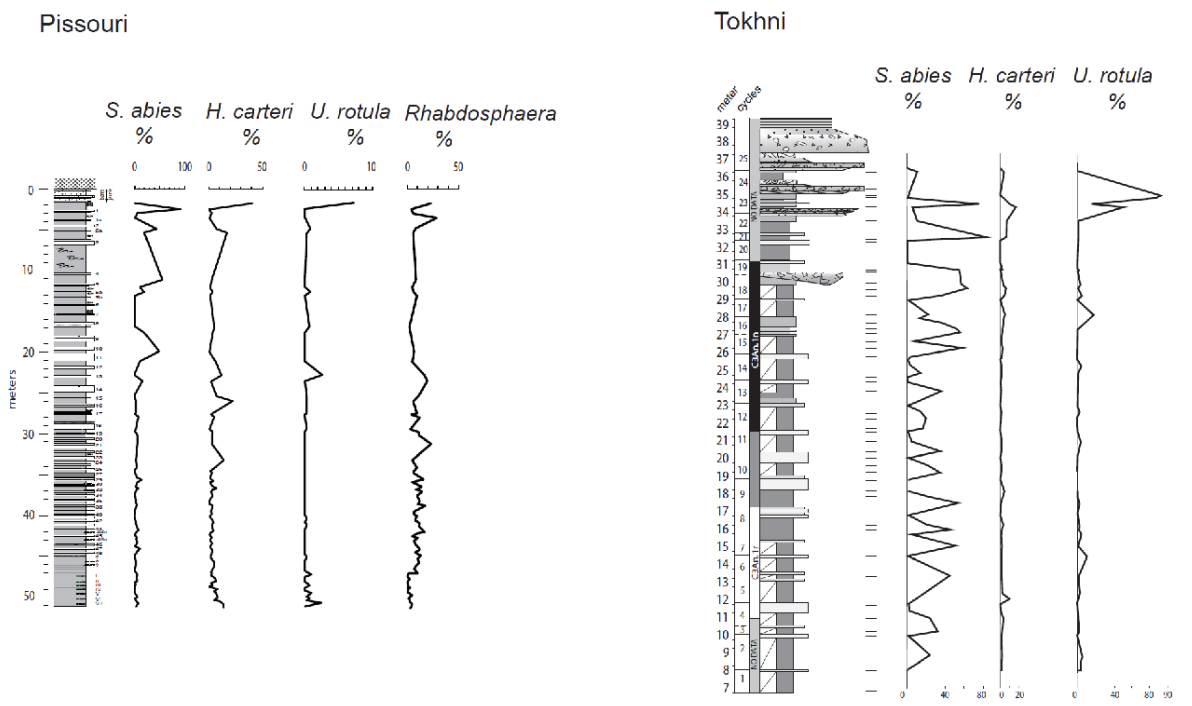

Fig. 4. Selected calcareous nannofossils relative abundance for the Tokhni and Pissouri sections, Cyprus.

At Tokhni, in the Psematismenos-Maroni Basin, where the lithologic cycles are characterized by the cyclic alternation of reddish shales and whitish micritic limestones (sometimes associated to or replaced by pink diatomites), *S. abies* is almost absent in all limestone layers, but shows greater abundance in the (sapropel equivalent) marly hemicycles from the base of the section, about 6.45 Ma, up to 5.95 Ma, with major peaks ranging from 29% to 83% of the assemblage (Gennari et al., 2018). Here the last major *S. abies* peak abundance (72% at 35.7 m) is accompanied by the remarkable high abundance of *H. carteri* (up to 16%) which in turn is followed by the *U. rotula* peak (90%), approximately at 36.15 m. In this section, no *Rhabdosphaera* spp. peak abundance has been recorded. Despite the common high abundance of *S. abies* in most of the cycles, the succession of *H. carteri* and *U rotula* peaks is evident when compared to the lower abundance of

these species along the entire section (never exceeding 12% and 18%, respectively), and their stratigraphic position with respect to the *S. abies* peak at 35.7m.

Finally at Pissouri, where the sediments spanning the MSC onset consist of cyclic alternations of soft brown marls and indurated calcareous beds (Kouwenhoven et al., 2006); the calcareous nannofossil assemblage is moderately to poorly preserved, the diversity is generally low to moderate, and the abundance shows a considerable decrease between ~30 and ~10 m. Above 20 m the nannoflora is poorly preserved and very scarce. Some samples at 20 and 11 m show almost monospecific assemblages consisting of *S. abies*. The plot shown in this paper (Fig. 4) records again, however, a succession of events in which *S. abies* increases up to 95% at 2.5 m, shortly followed by *H. carteri* (40%), *U. rotula* (8%) and *Rhabdosphaera* spp. (22%) peaks at 1.9 m.

4. Discussion

4.1 Chronostratigraphic framework

All the studied sections are correlated to the reference sections for the Mediterranean Messinian (Fig. 5) by means of planktonic foraminifer biostratigraphy, cyclostratigraphy, magnetostratigraphy (Fanantello, Tokhni, and Pissouri sections) (Krijgsman et al., 1999, 2002, Kouwenhoven et al., 2006, Manzi et al., 2007, Morigi et al., 2007, Lozar et al., 2018; Gennari et al., 2018). In detail, the chronostratigraphic position of the suite of CN bioevents presented here is mainly based on three constraints: 1) the position of the *T. multiloba* LO, 2) the base of the reverse chron C3r position, 3) the first branching selenite (PLG6) position, that we will discuss in the following lines.

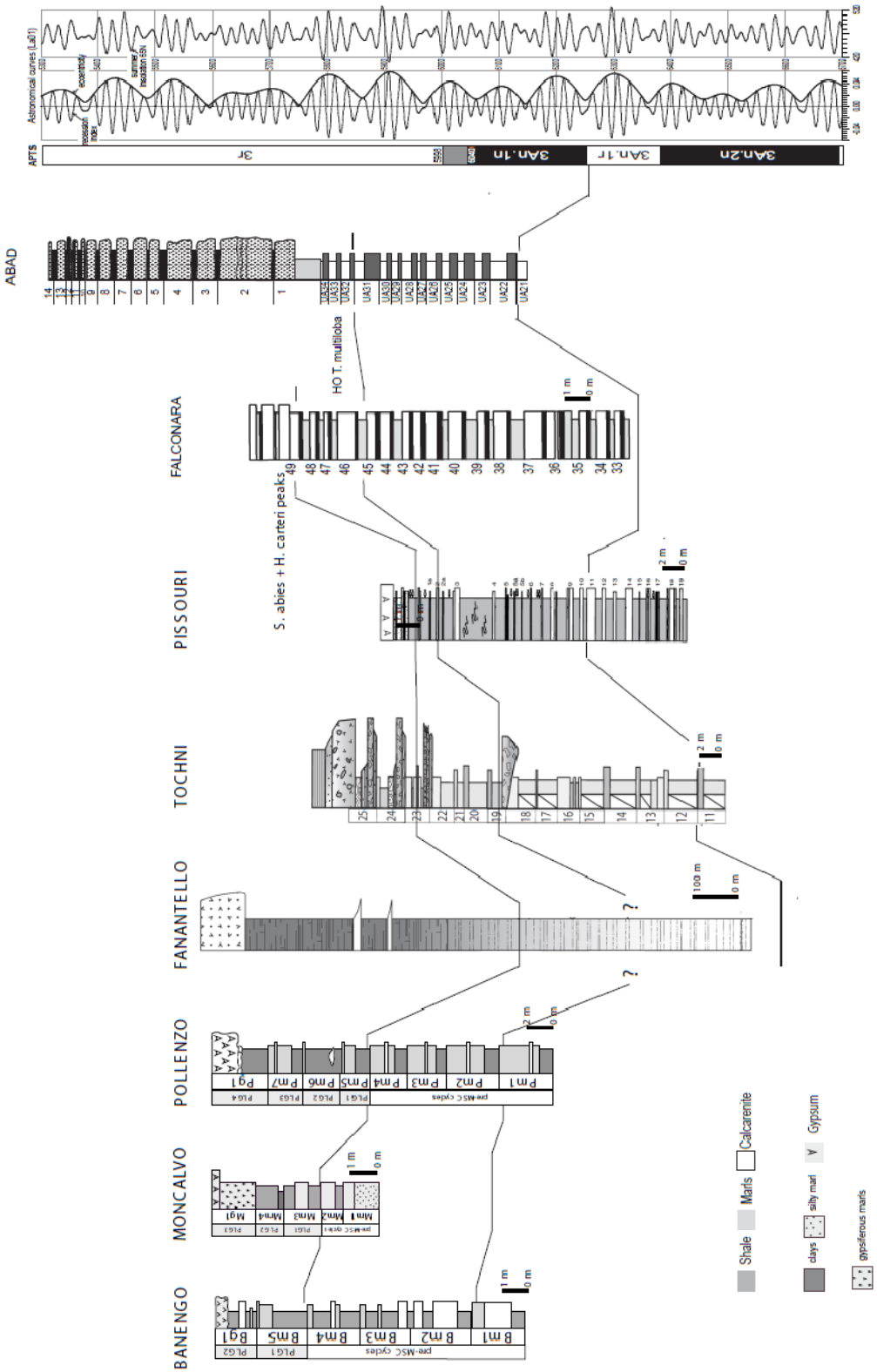
Astronomical curves (La91)
eccentricity
summer insolation 65N
precession index
APTS
3r
3An.1n
3An.1r
3An.2n
ABAD
HO T. multilloba
S. abies + H. carteri peaks
FALCONARA
PISSOURI
TOCHNI
FANANTELLO
POLLENZO
MONCALVO
BANENGO
pre-MSC cycles
Shale
Marls
Calcarenite
clays
silty marl
Gypsum
gypsiferous marls

Fig. 5. correlation of the studied sections to the Falconara and Abad reference sections (form Blanc-Valleron et al., 2002 and Sierro et al., 2001 respectively) by means of magnetostratigraphy, CN and PF datums.

1) the position of *T. multiloba LO*. *T. multiloba* is an endemic taxon that characterizes the Mediterranean Basin sedimentary record during the Messinian; its FO occurs at 6.415 Ma in the Abad section; its LO is recorded in cycle UA31 in the same section (Sierro et al., 2001, 2003). and cycle 45 in the Falconara-Gibliscemi section (Hilgen and Krijgsman, 1999; Blanc-Valleron et al., 2002), with an age range of 6.04 - 6.08 Ma. Moreover, the *T. multiloba* LO is recorded at the top of the normal polarity Chron C3An.1n. This event is recorded in the PB (Pollenzo and Banengo sections) four precessional cycles below the *S. abies* and *H. carteri* peaks and it allows bed by bed correlation to the Mediterranean reference sections (Krjigsman et al., 1999). In the Tokhni section the *T. multiloba* LO occurs at 31 m, four cycles below the *S. abies* and *H. carteri* peaks, in the normal polarity interval correlated to Chron C3An.1n. The Pissouri section records this event at 5 m (PC 2a), in a uncertain polarity interval, correlated to Chron C3An.1n by means of calcareous plankton biostratigraphic data (Krijgsman et al., 2002). The cyclostratigraphic interpretation of the section confirms that this event occurs four precessional cycles below the *S. abies* and *H. carteri* peaks.

In the Fanantello section (Northern Apennines) the scattered occurrence of planktonic foraminifera did not allow the precise identification of the *T. multiloba* LO (Manzi et al., 2007).

The stratigraphic record of the Moncalvo section starts above this level.

2) the base of the reverse chron C3r position. As stated above, the *T. multiloba* LO occurs at the top of the normal Chron C3An.1n, just below the reversal (Sierro et al., 2001). In the Fanantello section the CN peaks here reported for the first time at 63m, occur in a reversed polarity interval correlated to Chron C3r; the exact position of the reversal is uncertain and has been placed on the grounds of planktonic foraminifer biostratigraphy and cyclostratigraphy in an uncertain polarity interval (the highest normal is at 73m). Moreover, the CN peaks occur close to the LO of all foraminifera recorded at 61 m; this is also in agreement with data from the Pollenzo (Violanti et al., 2013) and the Tokhni sections (Gennari et al., 2018).

3) the position of the first branching selenite (PLG6). In the first stage of the MSC, Primary Lower Gypsum unit, sixteen to seventeen shale/gypsum cycles are recorded across the Mediterranean area, showing remarkably similar lithofacies and allowing bed by bed correlation across the region (Lugli et al., 2010; Roveri et al., 2014). The first occurrence of the branching selenite facies is thus regarded as an isochronous event at the basin scale (Lugli et al., 2010). For the Moncalvo section (PB) the correlation to the Mediterranean reference sections is granted by the physical stratigraphic correlation based on the first occurrence of this gypsum facies further up in the section (Dela Pierre et al., 2016; Lozar et al., 2018). The CN peaks reported herein occur five precessional cycles below the first occurrence of the branching selenite facies, recorded in the Sturani Key Bed (SKB, Dela Pierre et al., 2011, 2016) and thus correlate to cycle PLG1 as in the other PB sections. This is also confirmed in the Pollenzo section (Dela Pierre et al., 2011). Among other sections considered here, Banengo, Pissouri, and Tokhni are truncated by the Messinian Erosional Surface (MES, Roveri et al., 2014) a few cycles above the CN

peaks, or do not record Primary Lower Gypsum due to the distal location of the section (Fanantello).

From the chronostratigraphic tie points presented above, it follows that the age of the suites of calcareous nannofossil bioevents here described, is supported by bed to bed correlation to the Mediterranean reference sections (Abad and Falconara), and closely approximates the MSC onset. The other proxy for this event is the Last Recovery of foraminifera, but this event has proven ambiguous, since it occurs at a different stratigraphic position in some sections across the basin (e.g., Govone: Dela Pierre et al., 2016; Serra di Falco and Ravanusa: Catalano et al., 2016).

In four out of the six sections considered in our paper (Pissouri, Kouwenhoven et al., 2006; Pollenzo and Banengo, Lozar et al., 2018; Tokhni, Gennari et al., 2018), the CN peaks occur in the fourth precessional cycle above the *T. multiloba* LO. In the sections where magnetostratigraphy is available (Fanantello, Pissouri, and Tokhni), the CN peaks occur above the base of Chron C3r. In the sections where the PLG unit records the first branching selenite (that is synchronous at the basin scale and occurs in the 6th PLG cycle, Lugli et al., 2010) the CN peaks occur five cycles below the appearance of this facies (Pollenzo and Moncalvo) (Fig.5).

4.2 Uniqueness of the *S. abies-H. carteri* peaks

Other sections from the literature, besides those here discussed, show nearly monospecific assemblages occurring in cyclical deposits of Messinian age. For instance the Falconara/Gibliscemi section shows alternating reddish and white laminites alternating with marls (Sprovieri et al., 1996; Blanc-Valleron et al., 2002). Calcareous nannofossil assemblages are less diversified in the marls than in the

reddish and white laminites and the authors in particular observe nearly monospecific *S. abies* assemblages, which become very abundant in the pinkish laminites and reach the highest values just at the base of the white diatomite.

Some interesting peaks, exceeding 40% in abundance, are in particular seen at 6.665, 6.125, 6.11, 6.09, 6.065, and 6.015 Ma (respectively cycles 16, 43, 44, 45, 46, and 48; Blanc-Valleron et al., 2002). Unfortunately, Blanc-Valleron et al. (2002) did not report information on other relevant CN species, such as *H. carteri*. The calcareous nannofossil assemblages of this section were previously studied by Sprovieri et al. (1996, Fig. 3), showing that the upper *S. abies* peak occurs just below the “Calcare di base” (interpreted as the lithologic signature of the MSC onset), a few meters above the LO of *T. multiloba*, and is shortly followed by a sharp *H. carteri* peak (both around 100% of the total assemblage). Even if the two studies used the same sampling set, their correlation is neither easily achieved, nor discussed by the younger paper.

Sphenolithus abies peaks have also been recorded in the sediments underlying the gypsum beds in the Kalamaki section (Karakitsios et al., 2017); here the last *S. abies* peak occurs in a lithologic interval 1.5 m thick, in a reverse magnetic polarity interval correlated to Chron C3r, about 7 m below the gypsum. Unfortunately only semiquantitative data are available for this section. However, it is worth noting that the 1.5 m thick interval recording the *S. abies* high abundance also records the highest occurrence of foraminifera, commonly used as a proxy for the MSC onset (see Gennari et al., 2018 and references therein).

The record of the Tokhni section, as reported above, also shows regular *S. abies* peaks in the shale of each cycle, but the abundance of *H. carteri* never exceeds 10% before the last *S. abies* peak; in this cycle, approximating the MSC onset, *S.abies*

reaches 60% in abundance, and *H. carteri* 20% (Gennari et al., 2018), comparable to the data recorded in the PB and Northern Apennines sections.

As discussed above, the *S. abies* peak approximating the MSC onset is always reported at the same level with (or slightly preceding) the *H. carteri* peak. Additional *S. abies* peaks (see Table 1), although occurring at older or younger levels, do not show the simultaneous *H. carteri* peak and because of this can be easily discerned. These two peaks are often (but not always) accompanied by two secondary bioevents, the *U. rotula* and *Rhabdosphaera* spp. peaks. Therefore, the occurrence of multiple *S. abies* peaks does not prevent the correct identification of the one approximating the MSC onset, that is always accompanied by the *H. carteri* peak, and by secondary peaks of *Umbilicosphaera* spp. and *Rhabdosphaera* spp.

The presence/absence of older *S. abies* peaks could be driven by certain paleoceanographic conditions occurring in different settings. This is particularly evident in the Cyprian sections, where Pissouri and Tokhni record respectively random or continuous *S. abies* peaks. These sections are only about 60 km apart and this distance does not justify a difference driven by SST changes, since, as suggested by the current knowledge, *Sphenolithus* spp. was a warm water taxon (Perch Nielsen, 1985, Gibbs et al., 2004). On the contrary, the SST could instead exert a control on the *S. abies* relative abundance in the northern sections (e.g., Fanantello and Pollenzo), but evidently is not the exclusive one. Other paleoenvironmental drivers might be searched for in the Atlantic-Mediterranean connection, that was severely restricted at the onset of the MSC.

The occurrence of *Umbilicosphaera* spp. and *Rhabdosphaera* spp. seam to be particularly abundant in the upper part of the precessional cycle (Lozar et al.,

2018), correlated to minimum insolation. The occurrence of high abundance of these additional taxa, or on the contrary their local absence (*Umbilicosphaera*: Fanantello; *Rhabdosphaera*: Moncalvo and Fanantello), may indicate a more regional control. *Umbilicosphaera* spp. and *Rhabdosphaera* spp. are thus here regarded as secondary bioevents, in strong relation to water masses. We strongly encourage people to study these often neglected species which probably hide a paleoenvironmental meaning worthy to be explored.

5. Conclusions

We conclude that in the six sections considered in this paper, *S. abies* and *H. carteri* peaks approximate the MSC onset as supported by bed to bed correlation to the Mediterranean reference sections (Abad and Falconara). These bioevents are surely related to the environmental changes driven by the Mediterranean paleoceanographic evolution during the Messinian, however are worth to be further explored in sedimentary sections recording the MSC onset. In fact, the succession of *S. abies* and *H. carteri* peaks might represent an excellent correlation tool at the basin scale and although in the easternmost and southern sections several sphenolith peaks can be observed, the coupled *S. abies* and *H. carteri* increase is recorded only approximately at the MSC onset . Two secondary events, recorded in most sections, namely the *U. rotula* and *Rhabdosphaera* spp. peaks, are also helpful to approximate the MSC onset. We suggest that this suite of CN bioevents offers the possibility of overcoming correlation difficulties due to different sedimentary records or lack of magnetic signal (e.g., Fanantello, Pissouri, Tokhni sections).

Further investigation is needed in the Western Mediterranean Basin, for which detailed CN biostratigraphy is available so far only for narrow Messinian intervals (Flores et al., 2005).

Acknowledgement

We thank two anonymous reviewers for their constructive comments and the editorial handling by Richard Jordan. This research received MIUR funding to Alessandra Negri (AN) and Francesca Lozar.

REFERENCES

Bellanca, A., Caruso, A., Ferruzza, G., Neri, R., Rouchy, J.M., Sprovieri, M., 2001. Transition from marine to hypersaline conditions in the Messinian Tripoli Formation from the marginal areas of the central Sicilian Basin. Sedimentary Geology 140, 87-105.

Blanc-Valleron, M.M., Pierre, C., Caulet, J.P., Caruso, A., Rouchy, J.M., Cespuglio, G., Sprovieri, R., Pestrea, S., Di Stefano, E., 2002. Sedimentary, stable isotope and micropaleontological records of paleoceanographic change in the Messinian Tripoli Formation (Sicily, Italy). Palaeogeography, Palaeoclimatology, Palaeoecology 185, 255-286.

Bown, P.R., Young, J.R., 1998. Techniques. In: Bown P.R. (ed.), Calcareous Nannofossil Biostratigraphy. British Micropalaeontological Society Series, Chapman and Hall, London: 1-15.

Catalano, R., Di Stefano, E., Sprovieri, R., Lena, G., Valenti, V., 2016. The barren Messinian Tripoli in Sicily and its palaeoenvironmental evolution: suggestions on the exploration potential. Petroleum Geoscience 22 (4), 322-332.

Dela Pierre, F., Bernardi, E., Cavagna, S., Clari, P., Gennari, R., Irace, A., Lozar, F., Lugli, S., Manzi, V., Natalicchio, M., Roveri, M., Violanti, D., 2011. The record of the Messinian salinity crisis in the Tertiary Piedmont Basin (NW Italy): the Alba section revisited. Palaeogeography, Palaeoclimatology, Palaeoecology 310, 238-255.

Dela Pierre, F., Natalicchio, M., Lozar, F., Bonetto, S., Carnevale, G., Cavagna, S., Colombero, S., 2016. The northernmost record of the Messinian Salinity Crisis (Piedmont Basin, NW Italy). Field Trip Guide, RCMNS Interim Colloquium, Torino, 2014. Geological Field Trips, 8 (2.1), 1-58.

Drury, A.J., Lee, G.P., Gray, W.R., Lyle, M., Westerhold, T., Shevenell, A.E., John, C.M., 2018. Deciphering the State of the Late Miocene to Early Pliocene Equatorial Pacific. Paleoceanography and paleoclimatology 33, 246-263.

Flecker, R., Krijgsman, W., Capella, W., de Castro Martíns, C., Dmitrieva, E., Mayser, J.P., Marzocchi, A., Modestou, S., Ochoa, D., Simon, D., Tulbure, M., van den Berg, B., van der Schee, M., de Lange, G., Ellam, R., Govers, R., Gutjahr, M., Hilgen, F., Kouwenhoven, T., Lofi, J., Meijer, P., Sierro, F.J., Bachiri, N., Barhoun, N., Alami, A.C., Chacon, B., Flores, J.A., Gregory, J., Howard, J., Lunt, D., Ochoa, M., Pancost, R., Vincent, S., Yousfi, M.Z., 2015. Evolution of the Late Miocene Mediterranean-Atlantic gateways and their impact on regional and global environmental change. Earth-Science Reviews 150, 365-392.

Flores, J.A., Sierro, F.J., Glacon, G., 1992. Calcareous plankton analysis in the pre-evaporitic sediments of the ODP site 654 (Tyrrhenian Sea, Western Mediterranean). Micropaleontology 38 (3), 279-288.

Flores, J.-A., Sierro, F.J., Filippelli, G.M., Bárcena, M.A., Pérez-Folgado,M., Vázquez, A., Utrilla, R., 2005. Surface water dynamics and phytoplankton communities during deposition of cyclic late Messinian sapropels sequences in the western Mediterranean. Marine Micropaleontology 56, 50-79.

Gennari, R., Manzi, V., Angeletti, A., Bertini, A., Biffi, U., Ceregato, A., Faranda, C., Gliozzi, E., Lugli, S., Menichetti, E., Rosso, A., Roveri, M., Taviani, M., 2013. A shallow water record of the onset of the Messinian salinity crisis in the Adriatic foredeep (Legnagnone section, Northern Apennines). Palaeogeography, Palaeoclimatology, Palaeoecology 386, 145-164.

Gennari, R., Lozar, F., Turco, E., Dela Pierre, F., Manzi, V., Natalicchio, M., Lugli, S., Roveri, M., Schreiber, C., Taviani, M., 2018. Integrated stratigraphy and paleoceanographic evolution of the pre-evaporitic phase of the Messinian salinity crisis in the Eastern Mediterranean as recorded in the Tokhni section (Cyprus island). Newsletters on Stratigraphy 50, 1-23.

Hilgen, F.J., Krijgsman, W., 1999. Cyclostratigraphy and astrochronology of the Tripoli diatomite formation (pre-evaporite Messinian, Sicily, Italy). Terra Nova 11, 16-22.

Hilgen, F. J., Iaccarino, S., Krijgsman, W., Villa, G., Langereis, C. G., Zachariasse, W. J., 2000. The Global Boundary Stratotype Section and Point (GSSP) of the Messinian Stage (uppermost Miocene). Episodes, 23 (3), 172-178.

Karakitsios, V., Roveri, M., Lugli, S., Manzi, V., Gennari, R., Antonarakou, A., Triantaphyllou, M., Agiadi, K., Kontakiotis, G., Kafousia, N., De Rafelis, M., 2017. A record of the Messinian salinity crisis in the eastern Ionian tectonically active domain (Greece, eastern Mediterranean). Basin Research 29 (2), 203-233.

Kouwenhoven, T.J., Seidenkrantz, M.S., van der Zwaan, G.J., 1999. Deep-water changes: the near-synchronous disappearance of a group of benthic foraminifera from the Late Miocene Mediterranean. Palaeogeogr. Palaeoclimatol. Palaeoecol. 152 (3-4), 259-281-.

Kouwenhoven T.J.,Morigi C., Negri A., Giunta S. Krijgsman W., Rouchy J.M., 2006. Paleoenvironmental evolution of the eastern Mediterranean during the Messinian: Constraints from integrated microfossil data of the Pissouri Basin (Cyprus). Marine Micropaleontology 60, 17-44.

Krijgsman, W., Hilgen, F.J., Raffi, I., Sierro, F.J., Wilson, D.S., 1999. Chronology, causes and progression of the Messinian salinity crisis. Nature 400, 652–655.

Krijgsman, W., Blanc-Valleron, M.M., Flecker, R., Hilgen, F.J., Kouwenhoven, T.J., Merle, D., Orszag-Sperber, F., Rouchy, J.M., 2002. The onset of the Messinian salinity crisis in the Eastern Mediterranean (Pissouri Basin, Cyprus). Earth Planetary Science Letters 194 (3-4), 299-310.

Krijgsman W., Capella W., Simon D., Hilgen F.J., Kouwenhoven T.J., Meijer P.T., Sierro F.J., Tulbure M.A., van den Berg B.C.J., van der Schee M., Flecker R., 2018. The Gibraltar Corridor: Watergate of the Messinian Salinity Crisis. Marine Geology 403, 238-246.

Iaccarino, S., Salvatorini, G., 1982. A framework of planktonic foraminiferal biostratigraphy for Early Miocene to Late Pliocene Mediterranean area. Paleontologia Stratigrafia ed Evoluzione 2, 115-125.

Laskar, J., Robutel, P., Joutel, F., Gastineau, M.,Correia, A.C.M., Levrard, B., 2004. A long term numerical solution for the insolation quantities of the Earth. Astronomy and Astrophysics 428, 261-285.

Lozar, F., Violanti, D., Dela Pierre, F., Bernardi, E., Cavagna, S., Clari, P., Irace, A., Martinetto, E., Trenkwalder, S., 2010. Calcareous nannofossils and Foraminifers herald the Messinian salinity crisis: the Pollenzo section (Alba, Cuneo; NW Italy). Geobios 43, 21–32.

Lozar, F., Violanti, D., Bernardi, E., Dela Pierre, F., Natalicchio, M., 2018. Identifying the onset of the Messinian salinity crisis: a reassessment of the biochronostratigraphic tools (Piedmont Basin, NW Italy). Newsletters on Stratigraphy, 51 (1), 11-31.

Lugli, S., Manzi, V., Roveri, M., Schreiber, B. C., 2010. The Primary Lower Gypsum in the Mediterranean: a new facies interpretation for the first stage of the Messinian salinity crisis. Palaeogeography, Palaeoclimatology, Palaeoecology 297, 83–99.

Manzi V., Roveri M., Gennari R., Bertini A., Biffi U., Giunta S., Iaccarino S., Lanci L., Lugli S., Negri A., Riva A., Rossi M.E. and Taviani M.. 2007. The deep-water counterpart of the Messinian Lower Evaporites in the Apennine foredeep: The Fanantello section (Northern Apennines, Italy). Palaeogeography, Palaeoclimatology, Palaeoecology 251 (3-4), 470-499.

Manzi V., Lugli S., Roveri M., Schreiber, C., Gennari R., 2011. The Messinian “Calcare di Base” (Sicily, Italy) revisited. GSA Bulletin; 123 (1-2), 347-370.

Manzi, V., Gennari, R., Hilgen, F., Krijgsman, W., Lugli, S., Roveri, M., Sierro, F.J., 2013. Age refinement of the Messinian salinity crisis onset in the Mediterranean. Terra Nova 25 (4), 1-8.

Morigi C., Negri A., Giunta S., Kouwenhoven T., Krijgsman W., Blanc-Valleron M., Orszag-Sperber F., Rouchy J.M.. 2007. Integrated quantitative biostratigraphy of the latest Tortonian–early Messinian Pissouri section (Cyprus): An evaluation of calcareous plankton bioevents. Geobios 40, 267-279.

Negri, A., Villa, G., 2000. Calcareous nannofossil biostratigraphy, biochronology and palaeoecology at the Tortonian/Messinian boundary of the Faneromeni section (Crete). Palaeogeography, Palaeoclimatology, Palaeoecology 156 (3-4), 195-209.

Negri, A., Giunta, S., Hilgen, F., Krijgsman, W., Vai, G.B., 1999. Calcareous nannofossil biostratigraphy of the M. del Casino section (northern Apennines, Italy) and palaeoceanographic conditions at times of Late Miocene sapropel formation. Marine Micropalaeontology 36 (1), 13-30.

Ochoa, D., Sierro, F.J., Lofi, J., Maillard, A., Flores, J.A., Suarez, M., 2015. Synchronous onset of the Messinian evaporite precipitation: First Mediterranean offshore evidence. Earth and Planetary Science Letters 427, 112-124.

Raffi, I., Mozzato, C. A., Fornaciari, E., Hilgen, F. J., Rio, D., 2003. Late Miocene calcareous nannofossil biostratigraphy and astrobiochronology for the Mediterranean region. Micropaleontology 49, 1-26.

Pellegrino, L., Dela Pierre, F., Natalicchio, M., Carnevale, G., 2018. The Messinian diatomite deposition in the Mediterranean region and its relationships to the global silica cycle. Earth-Science Reviews 178, 154-176.

Roveri, M., Flecker, R., Krijgsman, W., Lofi, J., Lugli, S., Manzi, V., Sierro, F. J., Bertini, A., Camerlenghi, A., de Lange, G. J., Govers, R., Hilgen, F. J., Hübscher, C., Meijer, P.T., Stoica, M., 2014. The Messinian Salinity Crisis: past and future of a great challenge for marine sciences. Marine Geology 352, 25-58.

Sierro, F.J., Hilgen, F.J., Krijgsman, W., Flores, J.A., 2001. The Abad composite (SE Spain): a Messinian reference section for the Mediterranean and the APTS. Palaeogeography, Palaeoclimatology, Palaeoecology 168 (1-2), 141-169.

Sierro, F.J., Flores, J.A., Frances,G.,Vazquez, A.,Utrilla, R., Zamarreño, I., Erlenkeuser, H., Barcena, M.A., 2003. Orbitally-controlled oscillations in planktic communities and cyclic changes in western Mediterranean hydrography during the Messinian. Palaeogeography, Palaeoclimatology, Palaeoecology 190, 289-316.

Theodoridis, S., 1984. Calcareous nannofossil biostratigraphy of the Miocene and revision of the helicoliths and discoasters. Utrecht Micropaleontological Bulletin 32, 1-271.

Van den Berg, B.C.J., Sierro, F.J., Hilgen, F.J., Flecker, R., Larrasoaña, J.C., Krijgsman, W., Flores, J.A., Mata, M.P., 2018. Imprint of Messinian Salinity Crisis events on the Spanish Atlantic margin. Newsletters on Stratigraphy 51 (1), 93-115.

Violanti, D., Lozar, F., Dela Pierre, F., Natalicchio, M., Bernardi, E., Clari, P., Cavagna, S., 2013. Stress tolerant microfossils of a Messinian succession from the northern Mediterranean basin (Pollenzo section, Piedmont, Northwestern Italy). Bollettino della Società Paleontologica Italiana 52 (1), 45-54.

Wade, B.S., Bown P.R., 2006. Calcareous nannofossils in extreme environments: The Messinian Salinity Crisis, Polemi Basin, Cyprus. Palaeogeography, Palaeoclimatology, Palaeoecology 233, 271-286.

Young, J.R., 1998. Neogene. In: Bown, P.R. (Editor), Calcareous Nannofossil Biostratigraphy. British Micropalaeontological Society Publications Series. Chapman & Hall, London, pp. 225-265.

Figure captions

Fig. 1. Geographic location of the studied sections. 1: Fanantello, Northern Apennines (Italy); 2: Tokhni and Pissouri, Cyprus; 3: Pollenzo, Banengo and Moncalvo, Piedmont Basin, Italy).

Fig. 2. Selected Calcareous Nannofossil relative abundances and correlation of the Piedmont Basin sections by means of calcareous nannofossil and planktonic foraminifera datums (Data from Lozar et al., 2018).

Fig. 3. Selected calcareous nannofossil relative abundance for the Fanantello section.

Fig. 4. Selected calcareous nannofossil relative abundance for the Tokhni and Pissouri sections, Cyprus.

Fig. 5. Correlation of the studied sections to the Falconara and Abad reference sections (form Blanc-Valleron et al., 2002 and Sierro et al., 2001 respectively) by means of magnetostratigraphy, CN and PF datums.

Table 1. Inferred age of the Sphenolith peaks described in this paper in selected sections across the Mediterranean region.

Table 1

Section	Lithological	Inferred Age I	Inferred Age II	Inferred Age

	markers	peak, in Ma	peak, in Ma	III peak, in Ma
Banengo	PLG1 Equivalent	5.983-5.974		
Pollenzo	PLG1 Equivalent	5.983-5.974		
Moncalvo	PLG1 Equivalent	5.983-5.974		
Fanantello	PLG1 Equivalent	5.970	5.950	5.850
Pissouri	Below PLG	5.999		
Tokhni	PLG1	5.983-5.974		